Wood Sci Technol (2005) 39:
DOI 10.1007/s00226-005-0022-0

ORIGINAL

Marjan Sedighi-Gilani · Homeira Sunderland · Parviz Navi

Microfibril angle non-uniformities within normal and compression wood tracheids

Received: 18 May 2004 / Published online: 10 August 2005

Abstract The pattern and extent of variation of microfibril angle (MFA) in normal and compression tracheids of softwood were investigated by using confocal laser scanning microscopy technique. All measurements support the idea that the orientation of microfibrils in single wood tracheids is not uniform. MFA of the radial wall of earlywood tracheids was highly non-uniform and had an approximately circular form of arrangement around the bordered pits (inside the border). Between the bordered pits the measured MFAs were less than the other parts of the tracheid. In the latewood tracheids MFA was less variable. The average orientation of simple pits in the crossfield region was consistent with the mean MFA of the tracheids; however some of the measurements showed a highly variable arrangement in the areas between the simple pits. In many cases the local measured MFAs of compression wood tracheids agreed with the orientation of natural helical cavities of compression wood. Comparing the measured results in different growth rings showed that MFAs in juvenile wood are generally larger than in perfect wood.

Introduction

The major part of tracheid walls consist of the cellulose microfibrils, which are embedded helically in the hemicellulose and lignin matrix. The angle between the direction of the cellulose microfibrils in different layers of tracheid wall and the longitudinal direction of the wood tracheid is called microfibril angle (MFA). MFA of S_2 layer, which is the thickest layer of the tracheid wall, has a predominant effect on the wood mechanical properties. Since a long time the mean MFA was estimated by different methods; X-ray diffraction (Lichtenegger et al. 1999), orientation of pit apertures (Hiller 1964; Cockrell 1974), soft-rot cavities (Khalili 1999; Anagnost et al. 2000), polarized light microscopy

M. Sedighi-Gilani · H. Sunderland · P. Navi (✉)
Institute of materials science, Ecole polytechnique Fédérale de Lausanne,
1015 Lausanne, Switzerland
E-mail: Parviz.Navi@epfl.ch

(Page 1969; El-Hosseiny and Page 1973), direction of crystals of iodine (Bailey and Vestal 1937; Senft and Bendtsen 1985) and confocal laser scanning microscopy (CLSM; Batchelor et al. 1997; Jang 1998).

Analyzing the local MFA in single wood tracheid using the soft-rot cavity method (Khalili et al. 2001; Anagnost et al. 2002), improved iodine method (Wang et al. 2001) and X-ray microdiffraction technique (Lichtenegger et al. 2003) showed the variation of MFA along one wood tracheid and especially in radial walls with bordered pits. Also, systematic MFA measurements in different annual rings show that MFA reduces from pith to bark (Khalili et al. 2001; Anagnost et al. 2002; Bergander et al. 2002) and there is no correlation between MFA and morphological features such as fiber width or thickness.

The interest in compression wood studies arises from its important effect on wood mechanical properties. High lignin contents (Côte and Day 1965), helical cavities in the cell wall (Timell 1978, 1983; Yoshizawa and Ideia 1987), large MFA (Färber et al. 2001; Bergander et al. 2002) and low mechanical properties, especially in wet condition (Sedighi-Gilani and Navi 2004) are the specifications of compression wood tracheids. However, the pattern of variation of MFA in one compression wood fiber, the role of helical cavities in the tracheid microstructure and the origin of high sensibility of tensile behavior to the humidity variation are not understood properly.

The objective of this study is to understand the comprehensive pattern of microfibrils in single softwood tracheids. By using CLSM, local MFAs were measured at different points in normal and compression single wood tracheids. Earlywood and latewood tracheids and tracheids from different growth rings were tested and MFA in special zones like around the bordered pits or inside the crossfield zones were measured. In compression wood the local measured MFAs were compared to the orientation of natural helical cavities.

Materials and methods

Small cubic pieces of normal and compression wood were saturated in deionized water to facilitate chipping very thin layers (100 μm) with microtome. To delignify the prepared chips, modified Franklin procedure (48 h maceration in a solution of five parts acetic acid, one part hydrogen peroxide and four parts distilled water) was used. After rinsing, the macerated tracheids were stained with 0.05% Congo red solution for 30 min at 70°C. The single dyed tracheids were peeled out one by one and placed on a microscope slide.

A Carl Zeiss LSM 310 Confocal laser scanning microscope, equipped with an argon laser (excitation at 488 nm) and a rotating half-wave plate turning the plane of polarization of the laser beam, was used for measurements. Observations were performed with an X60 oil-immersion objective with a numerical aperture of 1.4. To stop the movement of the immersed tracheids in oil, they were fixed by sticking their ends to the slide. The developed CLSM method by Jang was used for each measurement of MFA (Jang 1998). A small area of the tracheid wall (less than 50 μm^2) was chosen and scanned at each 10° over the plane of 180°. The changes of the fluorescent intensity I, in each step were plotted against the angle of polarization. The sinusoidal changes of fluorescent intensity fit the equation:

$$I = A\cos^2(P - \theta) + I_{\min} \quad (1)$$

where A is the amplitude of the curve, I is the difluorescence intensity, $I_{\min}$ is the minimum difluorescence intensity, θ is the mean MFA of the chosen area and P is the angle of excitation polarization. MFA of the chosen area were obtained by fitting the measured data (fluorescent intensities) to Eq. 1 (Fig. 1).

In each measurement, to ensure that the MFA was measured in the S_2 layer, the cross-sectional images of the tracheid close to the chosen area were scanned using blue excitation, 488 nm. Then the microscope current position was refocused on the middle of the upper wall thickness (Fig. 2a, b). As the S_2 layer is the thickest layer of the cell wall (making up about 70–80% of the wall thickness (Fengel 1969), we could be sure that measurement in the middle of the wall thickness is done in the S_2 layer.

MFAs in the radial wall, areas between the bordered pits, inside the border of the pits and in the tangential wall of more than 100 earlywood and latewood tracheids were studied. To measure the MFA in the tangential walls, the upper surfaces of tracheids which were placed cornerwise on the slide were pressed by the soft touch of a glass cover slip and two adjacent tangential and radial walls were flattened. The measured MFAs of the crossfield areas in earlywood and latewood tracheids were compared with the orientation of pit apertures in these areas.

Compression wood is a part of the stem which forms in the leeward side of leaning trunks. It could be found in many non-predictable positions of a tree trunk and be recognized by the change of color in the stem. To compare the MFA in normal and compression wood, tracheids from normal and compression wood parts of spruce and larch stems were studied. Helical cavities in the cell wall of compression wood tracheid are one of its inherence shape characteristics. The local measured MFAs were compared with the orientation of these helical cavities in the cell walls.

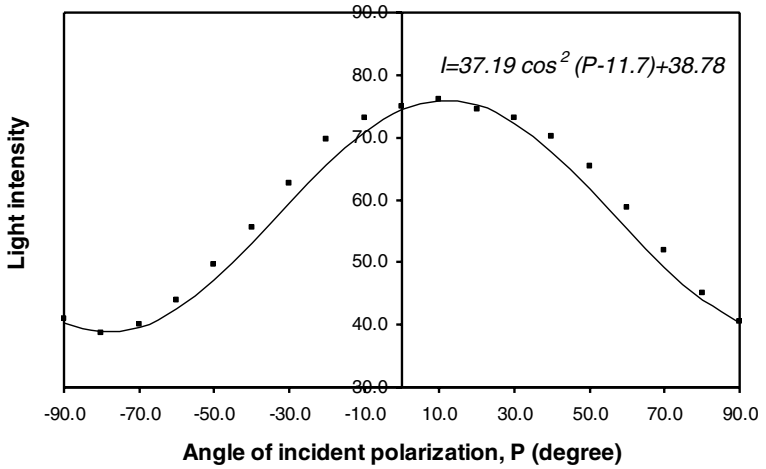

Fig. 1 Fluorescent intensity curve for the marked area in Fig. 2b. MFA = 11.7° gives the best fit to Eq. 1.

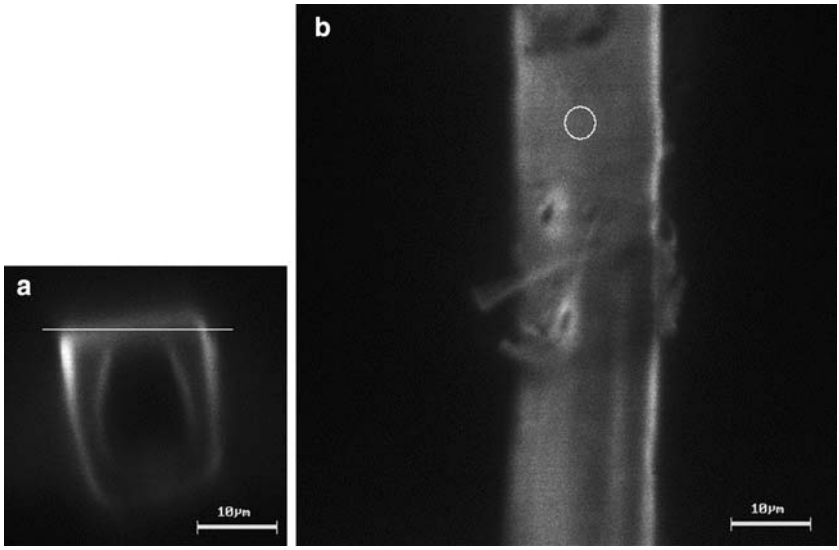

Fig. 2 Cross-sectional image and location of the focused area: (**a**) cross-sectional image of a latewood tracheid indicating the focused area is located in S_2 layer; (**b**) focused area for microscopic scanning.

Results and discussions

In this part the results of studying the MFA pattern in different tracheids of earlywood, latewood, juvenile wood, perfect wood and compression wood is presented.

Earlywood tracheids

Measurements of MFA in earlywood tracheids showed that MFA is considerably variable in the vicinities of the bordered pits on the radial walls. Measured MFAs between the bordered pits of earlywood tracheids were usually smaller than the mean MFA in non-pitted zones (Fig. 3a, b). Even the small negative values (relative to longitudinal axis) were often observed in the areas between two close pits.

This reduction of MFAs was limited to the central band of the radial wall (zones A) and out of this band the microfibrils followed the mean MFA of tracheid in non-pitted zones. MFAs of tangential wall in some areas close to the bordered pits of radial wall were measured (Fig. 4). Analyzing these measured MFAs showed that the high variation of MFAs was limited to the radial wall and the microfibrils orientation in the tangential walls is less variable. A closer look at the bordered pits area showed that the microfibrils had a deformed circular pattern of distribution around the pits and inside the borders (Fig. 5a, b). MFAs in the zones A and B have the same direction as mean MFA of the tracheid. But in the zones C and D, MFAs are negative relative to the tracheid longitudinal axis. In the zones E, F, G and H the measured MFAs have smaller values than the mean MFA of the tracheid (in this sample −5°, 13°, 8° and 10°

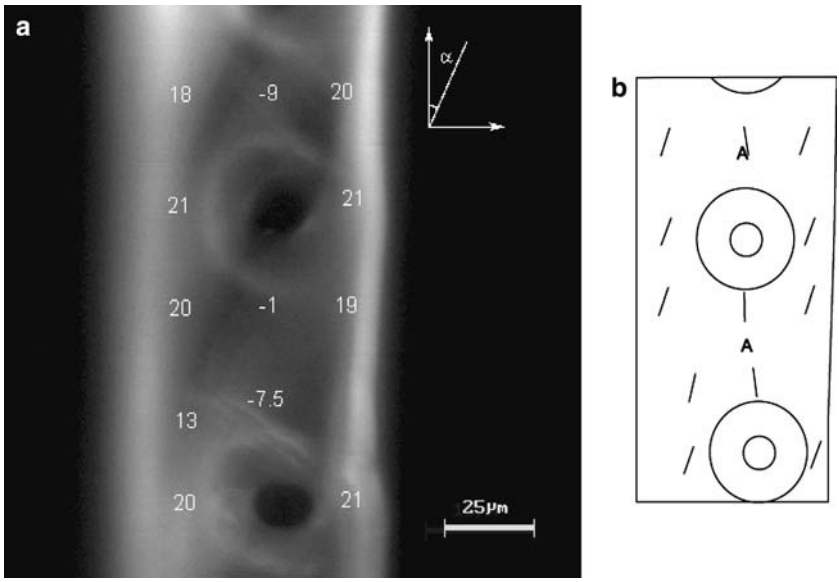

Fig. 3 Variation of MFA in the radial wall of an earlywood tracheid: (**a**) Measured MFAs and their locations; (**b**) plotted MFAs as measured in (**a**), reduction of the measured MFAs is limited to the central band of the radial wall which is marked as area *A*.

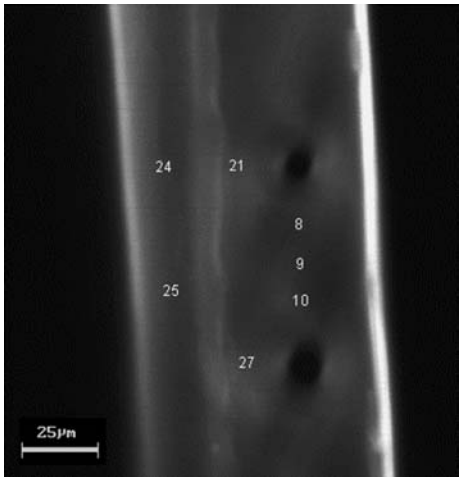

Fig. 4 Measured MFAs in tangential wall, radial wall and between two bordered pits.

in zones E and F). However when we measured the local angle of smaller areas like G_1, G_2, H_1 and H_2 larger values were obtained which were negative in zones H_1 and G_2 (42°, 72.5°) and positive in zones G_1 and H_2 (30.5°, 44.5°). The microfibrils approximate path which is plotted through these measured MFAs resembles the ''circular orientation'' of microfibrils which has been reported earlier (Harada 1965; Khalili et al. 2001), although it does not have a ''perfectly'' circular form.

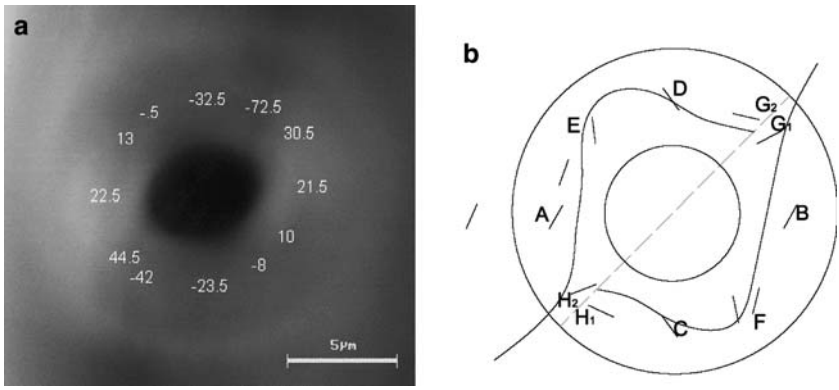

Fig. 5 Pattern of variation of MFA inside a bordered pit: (**a**) measured data; (**b**) schematic sketch.

In the central band of the earlywood radial wall the measured MFAs were always less than the mean MFA of the tracheid (Fig. 3a, b). Even the small negative values (relative to longitudinal axis) were common in this region. There are two possible eventualities to explain this phenomenon; existence of crossed microfibrils in this region (Fig. 6a) or unidirectional pattern of microfibrils (Fig. 6b). As microfibrils paths are not directly visible in CLSM method, it is not easy to say which eventuality is definitive. But frequent existence of the crossed microfibrils in the soft-rot fungi results, led us to doubt whether microfibrils in this zone have such pattern (Khalili et al. 2001). In an area with two planes of crossed microfibrils, in each step of measurement the measured fluorescent intensity is emitted from two different directions and the measured MFA would be the resultant of the two directions (Fig. 7).

The origin of the crossed microfibrils between the bordered pits could be explained by analyzing the variation of MFAs inside the border of bordered

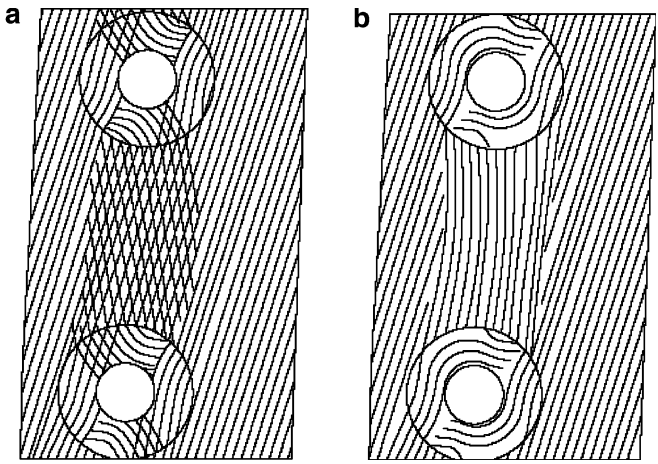

Fig. 6 Two proposed patterns of microfibrils between two bordered pits: (**a**) crossed microfibrils assumption; (**b**) unidirectional microfibrils assumption.

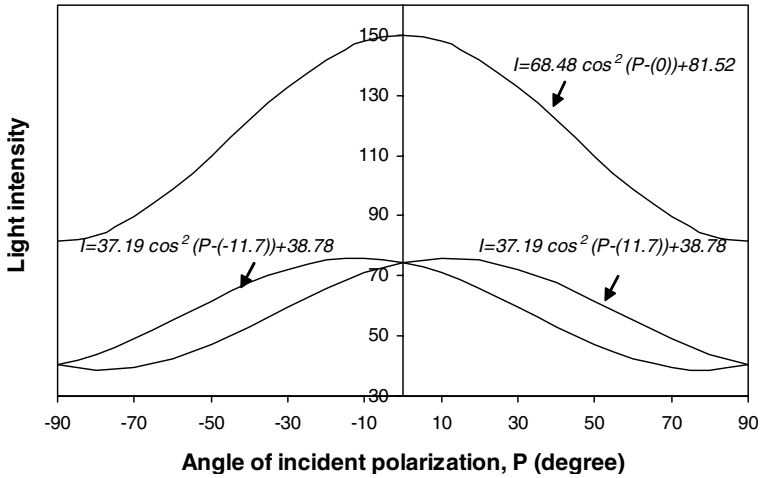

Fig. 7 Measured MFA (based on polarization) of an area with two crossed planes of microfibrils (MFA = 11.7°, −11.7°) is the resultant of the two directions (MFA = 0°).

pits (Fig. 5a, b). In most of the earlywood tracheids the measured MFAs in the top and bottom regions of the bordered pits had large negative values (S-helical direction). It is possible that the S-helical microfbrils inside the border continue over the pit border into the area between the two pits and coupling with the Z-helical microfibrils in this region making a crossed form. However, as direct observation of the cellulose microfibril paths is impossible with CLSM, the non-crossed unidirectional pattern of microfibrils cannot be rejected by this method. Measuring the local MFA of the small areas between the cross-field pits of earlywood tracheids usually showed uniform microfibrils distribution (Fig. 8a) and consistency with the orientation of pit apertures in this zone. However, in some of the tracheids the measured MFAs between the pits were variable and even turned to very small or negative values (Fig. 8b).

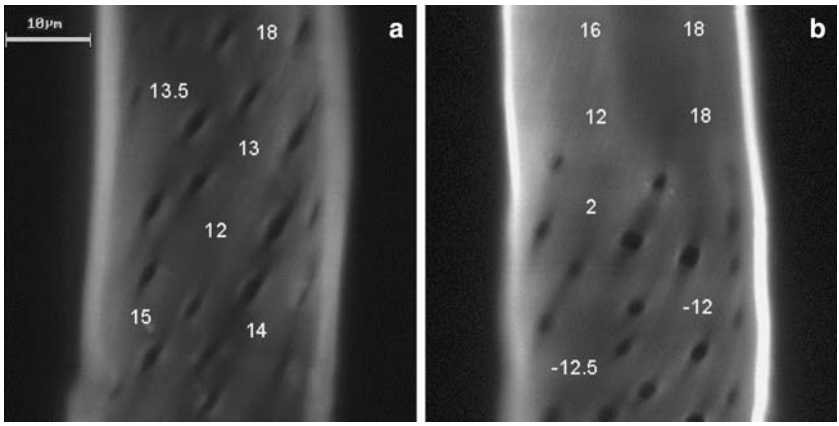

Fig. 8 Variation of MFA in cross-field region of two earlywood tracheids: (**a**) measured MFAs were not highly different; (**b**) MFAs were variable in different small areas between the pits.

Latewood tracheids

The MFA variation within the latewood tracheids was much smaller than the variation in earlywood tracheids. Even close to the steep narrow pits of the latewood tracheids (which have been usually observed adjacent to the ray cells) the parallel helical arrangement of microfibrils was approximately uniform (Fig. 9a, b).

Juvenile and perfect wood tracheids

In previous parts, MFAs of numerous wood tracheids taken from different parts of the stem (both juvenile and perfect wood) were tested. However, to understand the effect of juvenility on MFA, a comparative study in different growth rings was performed. Figure 10 shows the variation of MFA in the wood chips of rings 1–5 and 9–13 (juvenile wood), 24–32, 45–63 and 63–76 (perfect wood). Measured MFAs between bordered pits (which are always smaller than MFA in non-pitted areas) were ignored in this figure. MFA reduces from pith to bark although the variation of mean MFA in different rings is not substantial.

Compression wood

Figure 11 shows the variation of MFA close to the bordered pits of compression earlywood tracheids (spruce and larch). MFA between two close bordered pits is less than other local MFAs on the tracheid. Helical cavities of com-

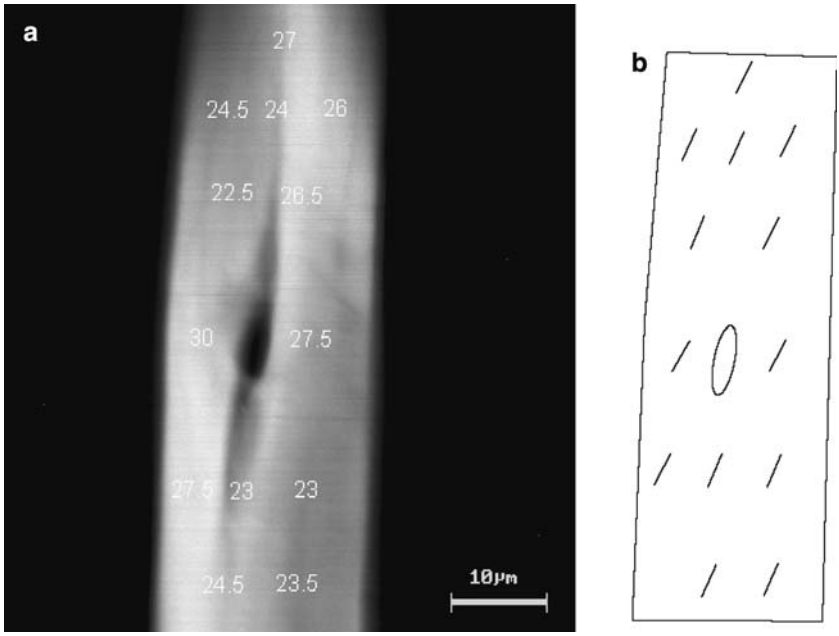

Fig. 9 MFA uniformity in latewood tracheids: (**a**) measured MFAs and their locations, (**b**) plotted MFAs as measured in (**a**).

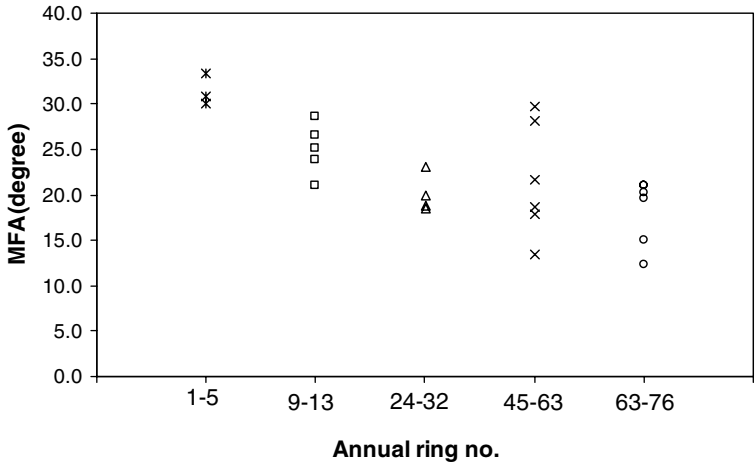

Fig. 10 MFA as a function of annual growth rings, measured in rings 1–5, 9–13, 24–32, 45–63 and 63–76.

pression earlywood tracheids are not as clearly visible as the latewood tracheids. However in the regions where the orientation of helical cavities is visible, these orientations are comparable with the measured local MFAs by CLSM. Figure 12 shows the relative agreement between the measured MFA and orientation of cavities in 12 spruce and larch latewood fibers.

In Fig. 13 the photos of two compression latewood tracheids (natural helical cavities are visible) and the measured local MFA are illustrated. The measured MFAs are almost the same as the orientation of helical cavities. MFA of compression larch tracheids in different growth rings were measured by X-ray diffraction technique (Fioravanti and Sodini 2005) and compared to the measured values by CLSM method (Table 1). Ring numbers 5–7 contained the compression wood tracheids and ring 4 was normal wood. Comparison of the

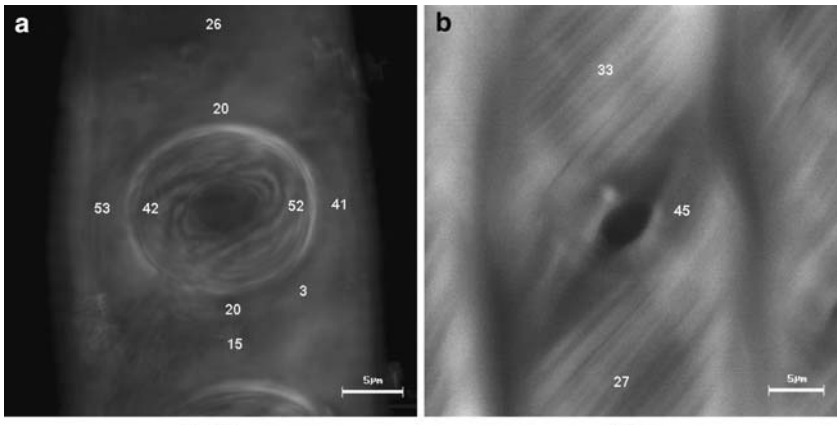

Fig. 11 MFA close to the bordered pits of compression earlywood tracheids.

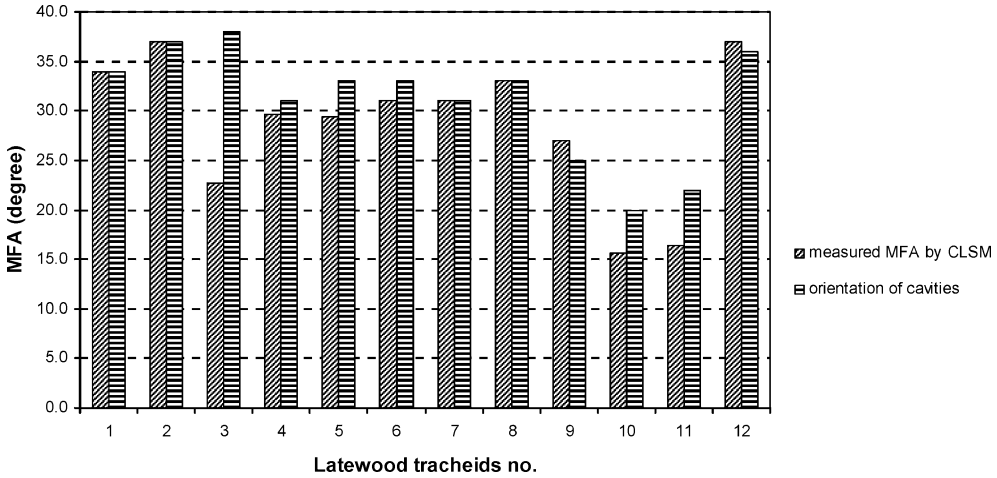

Fig. 12 Relative agreement between measured MFA of 12 spruce and larch compression latewood tracheids and the orientation of their helical cavities.

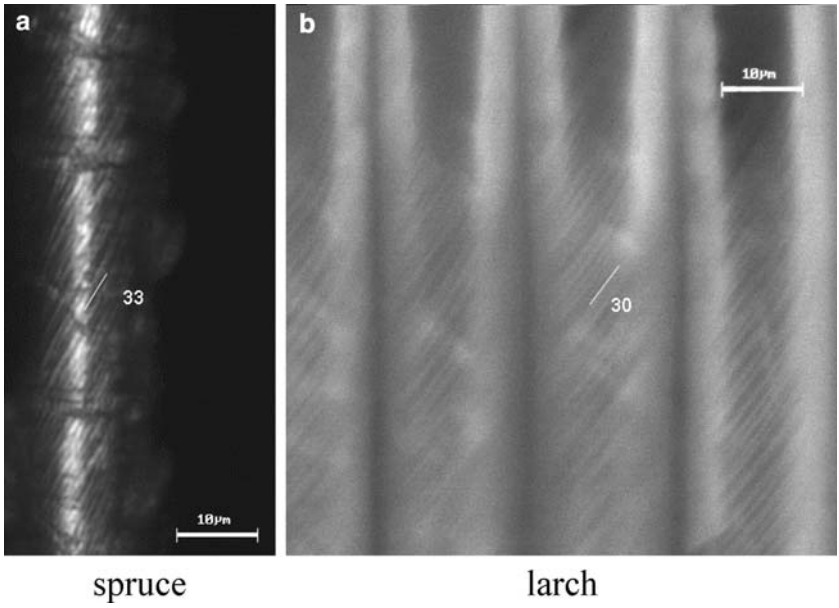

Fig. 13 Measured MFA in compression latewood tracheids, helical cavities of compression wood tracheids are visible.

results of measurements by X-ray diffraction technique and CLSM method shows some discrepancies. These discrepancies rise from the fact that in X-ray method the measured MFA corresponds to mean value of some adjacent wood tracheids, while in CLSM method a "local" MFA in S_2 layer of one tracheid is measured.

In Table 1, in CLSM columns, the local measured MFAs in some points along different tracheids of each ring were presented. The measured values

Table 1 Measured MFA by X-ray in different growth rings and CLSM local results in single tracheids of the same rings

Ring no.	Latewood		Earlywood	
	CLSM*	X-ray	CLSM*	X-ray
4	30, 33°	22°	13, 36, 33° Between bordered pits: 18, 5, 10.5°	26°
5	34, 37, 23, 30°	32°	45, 44, 49° Between bordered pits: 32, 26, 24°	37°
6	23, 30, 31°	31°	26° Between bordered pits: 21, 21, 18°	42°
7	37°	28°	56,61,54,47° Between bordered pits: 13, 12, 11, 52°	39°

*MFAs were measured in some different points along different tracheids of each ring.

between bordered pits of earlywood tracheids were considerably less than MFA in other parts of the fibers and confirmed the results of the former part.

Conclusions

CLSM was used to investigate the variation of MFA in individual tracheids. MFA were measured in different points of earlywood and latewood tracheids of compression wood and normal wood. Special zones like inside the border of the pits or cross-field zones were investigated by focusing on arbitrary small areas along the wood tracheids. MFA was highly variable within the radial wall of earlywood tracheids, especially in the vicinity of the bordered pits, and less variable in the latewood and tangential wall of earlywood tracheids. Measurements of MFA in different growth rings from pith to bark showed that MFA in juvenile wood is generally larger than in perfect wood. In compression wood MFA of earlywood and latewood tracheid were compared to the orientation of natural helical cavities in the cell walls. In many cases, the measured MFA in compression wood had a good agreement with these natural helical cavities. CLSM has the advantage to give the MFA of each area of the tracheid which is the subject of the study. Although measuring the MFA by CLSM is a laborious method, the mentioned characteristics make it a reliable technique for microstructural study of wood fibers.

Acknowledgment The financial support of the Swiss federal office of education and science in the framework of COST E20 and COST E35 is acknowledged with gratitude.

References

Anagnost SE, Mark RE, Hanna RB (2000) Utilization of soft-rot cavity orientation for the determination of microfibril angle. Part I. Wood Fiber Sci 32(1):81–87

Anagnost SE, Mark RE, Hanna RB (2002) Variation of microfibril angle within individual tracheids. Wood Fiber Sci 34(2):337–349

Bailey IW, Vestal MR (1937) The orientation of cellulose in the secondary wall of tracheary cells. Arnold Arbo 18:185–195

Batchelor WJ, Conn AB, Parker IH (1997) Measuring the fibril angle of fibers using confocal microscopy. Appita J 50:377–380

Bergander A, Brandstrom J, Daniel G, Salmen L (2002) Fibril angle variability in earlywood of Norway spruce using soft rot cavities and polarization confocal microscopy. J Wood Sci 48:255–263

Cockrell RA (1974) A comparison of latewood pits, fibril orientation and shrinkage of normal and compression wood of Giant Sequoia. Wood Sci Technol 8:197–206

Côte WA, Day AC (1965) Anatomy and ultrastructure of reaction wood. In: Côte WA Jr (ed.). Cellular ultrastructure of woody plants. Syracuse University, Syracuse NY, pp. 391–418
El-Hosseiny F, Page DH (1973) The measurement of fibril angle of wood fibers using polarized light. Wood Fiber Sci 5:208–214
Färber J, Lichtenegger HC, Reiterer A, Stanzl-Tschegg S, Fratzl P (2001) Cellulose microfibril angles in a spruce branch and mechanical implications. J Mat Sci 36:5087–5092
Fengel D (1969) The ultrastructure of cellulose from wood, Part I: wood as the basic material for the isolation of cellulose. Wood Sci Technol 3:203–217
Fioravanti M, Sodini N (2005) Personal communication. DISTAF-University of Florence, Italy
Harada H (1965) Ultrastructure and organization of gymnosperm cell walls. In: Côté WA Jr (ed.). Cellular ultrastructure of woody plants. Syracuse University Press, Syracuse NY, pp. 215–233
Hiller CH (1964) Correlation of fibril angle with wall thickness of tracheids in summerwood of slash and loblolly pine. TAPPI 47(2):125–128
Jang HF (1998) Measurement of fibril angle in wood fibres with polarization confocal microscopy. J Pulp Paper Sci 24:224–230
Khalili S (1999) Microscopic studies on plant fiber structure Department of Wood Science. Swedish University of Agricultural Sciences, Uppsala Sweden
Khalili S, Nilsson T, Daniel G (2001) The use of rot fungi for determining the microfibrillar orientation in the S2 layer of pine tracheids. Holz Roh- Werkst 58:439–447
Lichtenegger H, Reiterer A, Stanzl-Tschegg SE, Fratzl P (1999) Variation of cellulose microfibril angles in softwoods and hardwoods—a possible strategy of mechanical optimization. J Struct Biol 128:257–269
Lichtenegger HC, Müller M, Wimmer R, Fratzl P (2003) Microfibril angle inside and outside cross-fields of Norway spruce tracheids. Holzforschung 57:13–20
Page DH (1969) A method for determining the fibrillar angle in wood tracheids. J Microsc 90:137–143
Sedighi-Gilani M, Navi P (2004) Influence of wood fibers morphology on their non-linear behavior in axial tension. Third International Conference of the European Society for Wood Mechanics. Vila Real, Portugal
Senft JF, Bendtsen AB (1985) Measuring microfibrillar angles using light microscopy. Wood Fiber Sci 17:564–567
Timell T (1978) Ultrastructure of compression wood in Ginkgo biloba. Wood Sci Technol 12:89–103
Timell T (1983) Origin and evolution of compression wood. Holzforschung 37:1–10
Wang HH, Drummond JG, Reath SM, Hunt K, Watson PA (2001) An improved fibril angle measurement method for wood fibers. Wood Sci Technol 34:493–503
Yoshizawa N, Ideia T (1987) Some structural and evolutionary aspects of compression wood tracheids. Wood Fiber Sci 19:343–352